

# Biophysical characterization of the *Lactobacillus delbrueckii* subsp. *bulgaricus* membrane during cold and osmotic stress and its relevance for cryopreservation

Julie Meneghel<sup>1</sup> · Stéphanie Passot<sup>1</sup> · Sébastien Dupont<sup>2</sup> · Fernanda Fonseca<sup>1</sup>

Received: 21 July 2016 / Revised: 8 September 2016 / Accepted: 12 October 2016 / Published online: 31 October 2016  
© Springer-Verlag Berlin Heidelberg 2016

**Abstract** Freezing lactic acid bacteria often leads to cell death and loss of technological properties. Our objective was to provide an in-depth characterization of the biophysical properties of the *Lactobacillus delbrueckii* subsp. *bulgaricus* membrane in relation to its freeze resistance. Freezing was represented as a combination of cold and osmotic stress. This work investigated the relative incidence of increasing sucrose concentrations coupled or not with subzero temperatures without ice nucleation on the biological and biophysical responses of two strains with different membrane fatty acid compositions and freeze resistances. Following exposure of bacterial cells to the highest sucrose concentration, the sensitive strain exhibited a survival rate of less than 10 % and 5 h of acidifying activity loss. Similar biological activity losses were observed upon freeze-thawing and after osmotic treatment for each strain thus highlighting osmotic stress as the main source of cryoinjury. The direct measurement of membrane fluidity by fluorescence anisotropy was linked to membrane lipid organization characterized by FTIR spectroscopy. Both approaches made it possible to investigate the specific contributions of the membrane core and the bilayer external surface to cell degradation caused by cold and osmotic stress. Cold-induced membrane rigidification had no significant implication on bacterial freeze-thaw resistance. Interactions between

extracellular sucrose and membrane phospholipid headgroups under osmotic stress were also observed. Such interactions were more evident in the sensitive strain and when increasing sucrose concentration, thus suggesting membrane permeabilization. The relevance of biophysical properties for elucidating mechanisms of cryoinjury and cryoprotection is discussed.

**Keywords** Lactic acid bacteria · Freezing · FTIR spectroscopy · Membrane fluidity and organization · Phospholipid headgroups

## Introduction

Lactic acid bacteria (LAB) are widely used as starters for manufacturing fermented foods and probiotic products, as well as in green chemistry applications. LAB are delivered to food companies in the form of highly concentrated, ready-to-use products. The commercialization of starters requires production and preservation techniques that maximize the technological properties and shelf life of bacterial cells. Freezing is a widely used preservation technique, and very fast cooling rates (immersion in liquid nitrogen) are currently applied in industry. However, fast freezing requires low storage temperatures (~−50 °C for industrial application, ≤−80 °C for culture collection) and often leads to a degradation of the viability and acidifying activity upon thawing (Smittle et al. 1972; Fonseca et al. 2006). Bacterial resistance to freezing and to frozen storage depends on many parameters including the bacterial species, growth conditions, protective additives, freezing rate, and final storage temperature (Gomez Zavaglia et al. 2000; Fonseca et al. 2001). Applying slow cooling rates allows reproducible freezing protocols, but the biological

**Electronic supplementary material** The online version of this article (doi:10.1007/s00253-016-7935-4) contains supplementary material, which is available to authorized users.

✉ Fernanda Fonseca  
fonseca@grignon.inra.fr

<sup>1</sup> UMR GMPA, AgroParisTech, INRA, Université Paris-Saclay, 78850 Thiverval-Grignon, France

<sup>2</sup> Univ. Bourgogne Franche-Comté, AgroSup Dijon, PAM UMR A 02.102, 21000 Dijon, France

response of LAB during freezing still needs to be characterized and linked to bacterial freezing tolerance.

The major physical events that take place during slow freezing are well documented (Mazur et al. 1972; Fonseca et al. 2016). Firstly, during the chilling step applied after fermentation, membrane lipid phase transition may occur. Upon cooling, the phospholipid bilayer changes from a fluid and disordered liquid-crystalline phase to a rigid and ordered gel phase. This membrane solidification occurs at a temperature that mainly depends on cell type and growth conditions (Molina-Höppner et al. 2004; Ragoonanan et al. 2008; Gautier et al. 2013; Velly et al. 2014). Shortly thereafter or at the same time as the membrane lipid phase transition, water crystallizes and ice gradually forms in the extracellular matrix. No formation of intracellular ice was reported following LAB freezing in the presence of additives (Fonseca et al. 2006). The extracellular matrix becomes more and more concentrated and exerts an increasing osmotic pressure on the supercooled intracellular compartment. This osmotic gradient draws water out from the cells, leading to intracellular solute concentration. Cell dehydration and volume reduction proceed until the intracellular compartment reaches the maximal freeze concentration and forms a glassy state. Cells thus become osmotically irresponsive to the extracellular matrix (Fonseca et al. 2016). During the subsequent reduction in temperature, the extracellular matrix continues to evolve with the formation of ice and freeze concentration until it becomes a glass. After subsequent storage at low temperature, all these physical events are reversed during thawing before using LAB in industrial process.

The cell membrane is the primary target of damage following the sequential physical events previously described. Loss of membrane integrity, membrane permeabilization, and leakage of intracellular contents were reported following freezing at slow cooling rates (Fernández Murga et al. 2001; Rault et al. 2007; Moussa et al. 2008; Simonin et al. 2015). The severity of membrane damage is dependent on the temperature value at which these physical transitions occur during freezing. Gautier et al. (2013) reported that the membrane of LAB with low lipid transition temperature exhibited no loss of membrane integrity following freezing and thawing. This membrane property is strongly related to fatty acid (FA) composition, which could be modulated by modifying LAB culture conditions (Fernández Murga et al. 2000; Beal et al. 2001; Wang et al. 2005; Streit et al. 2008; Gautier et al. 2013). Furthermore, Fonseca et al. (2016) recently demonstrated that the freezing resistance of LAB could be improved by decreasing the glass transition temperature of the intracellular compartment by adding specific cryoprotective agents.

To limit freeze-thaw cellular damage, LAB concentrates are suspended in cryoprotective solutions. Disaccharides are non-penetrating cryoprotective agents (CPAs) usually used for LAB preservation (Hubálek 2003). Sugars are known for their contribution to cell stabilization. Cells are immobilized in a

sugar glassy matrix that strongly reduces the chemical and physical degradation reactions. Moreover, it has been reported that sugars exert a direct protective effect on membrane phospholipids and proteins (Crowe et al. 1988; Crowe et al. 1990; Santivarangkna et al. 2008). Although the exact interaction mechanism between sugars and membranes is still unclear, two principal theories have emerged: preferential exclusion and water replacement. In physiological conditions, phospholipid hydrophilic head groups are involved in hydrogen bonding with several water molecules (Luzardo et al. 2000). The first theory hypothesizes that CPAs are preferentially excluded from this hydration shell, thus reinforcing water hydrogen bonding to phospholipids. The second theory assumes a direct interaction between sugars and the membrane. According to this theory, sugars establish hydrogen bonds with phospholipid headgroups, thereby displacing the hydrating water molecules. Paradoxically, the addition of CPA also represents a source of osmotic stress for cells, especially as the extracellular medium cryoconcentrates. The freezing process may therefore be considered as a source of two major stresses for bacterial cells: cold and osmotic (Moussa et al. 2008; Simonin et al. 2015). To our knowledge, no study has yet focused on the individual contribution of exposure to cold temperatures and to increasing solute concentrations on the biological activity of LAB.

The aim of the present study was to better understand LAB cryoinjuries by analyzing the relative incidence of cold and osmotic stresses on the biological response and on the membrane properties of two strains of *L. bulgaricus* with different freeze resistances. Membrane biophysical properties were dynamically assessed during cooling and at incremental solute concentrations to mimic a freezing procedure. Membrane fluidity and lipid organization were investigated at the center and external surface of the phospholipid bilayers using spectrofluorimetry and FTIR spectroscopy, respectively.

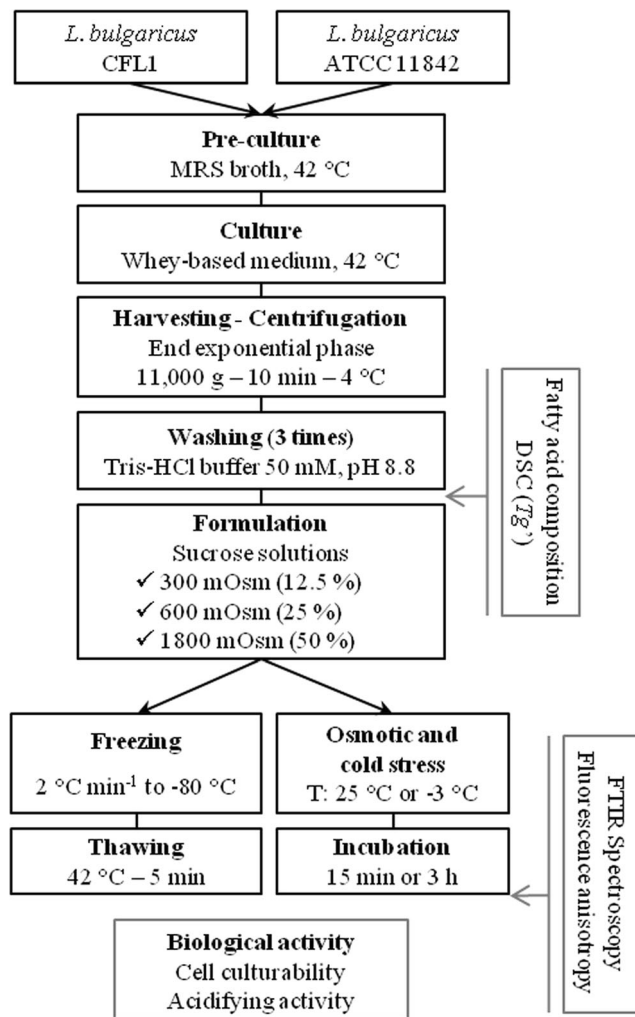
## Materials and methods

Figure 1 presents the experimental approach used in this study as well as the main parameters investigated. Unless otherwise specified, all measurements were performed from three independent bacterial cultures.

### Bacterial strains and culture conditions

Two strains of *Lactobacillus delbrueckii* subsp. *bulgaricus* were used in this study: *L. bulgaricus* CFL1 (CIRM-BIA; Rennes, France) and *L. bulgaricus* ATCC 11842 (Manassas, VA, USA).

Inocula were stored at  $-80\text{ }^{\circ}\text{C}$  and were thawed at  $42\text{ }^{\circ}\text{C}$  for 5 min before inoculation in 30 mL of MRS broth (Biokar Diagnostics; Beauvais, France). Preculture was carried out at



**Fig. 1** Diagram of the experimental approach used in the study and the main parameters investigated

42 °C up to the stationary growth phase. Approximately 150  $\mu\text{L}$  of the pre-culture was then used to inoculate 300 mL of Whey medium, and the culture was incubated at 42 °C until the end of the exponential growth phase (10 h for *L. bulgaricus* CFL1; 13 h for *L. bulgaricus* ATCC 11842) according to the procedure detailed by Gautier et al. (2013).

The Whey medium consisted of 60  $\text{g L}^{-1}$  mild whey powder (Euroserum; Port-sur-Saône, France) that was heated at 110 °C for 20 min. The supernatant obtained after centrifugation (17,000 $\times$ g for 30 min at 4 °C) and filtration was supplemented with 5  $\text{g L}^{-1}$  yeast extract (Organotechnie SAS; La Courmeuve, France) and sterilized at 110 °C for 20 min.

Absorbance measurements at 600 nm were regularly performed to adjust the culture time and the inoculation rate to guarantee harvest at the end of the exponential growth phase.

Cell cultures were cooled at 5 °C and harvested by centrifugation (11,000 $\times$ g for 10 min at 5 °C). Cell pellets were then washed three times in Tris-HCl buffer (50 mM, pH 8.8, BioRad; Hercules, CA, USA) in order to remove growth medium

constituents and excreted microbial metabolites that might negatively interfere with further analysis procedures.

### Freezing and thawing protocol

Washed cell pellets were resuspended in the same weight (1:1 ratio) of a sucrose solution (20 % wt. sucrose in saline water, corresponding to a value of osmolarity of 600  $\text{mOsm L}^{-1}$ , further referred to as mOsm). Cryotubes with a capacity of 2 mL were filled with 500  $\mu\text{L}$  of cryoprotected bacterial suspension and inserted into a controlled rate freezer (EF600–103, Asymptote; Cambridge, UK) precooled to 5 °C. The sample temperature was monitored by inserting a thermocouple (K type) into one cryotube. After a holding step of 10 min at 5 °C, the freezer was programmed to cool the sample device at 2 °C  $\text{min}^{-1}$ , from 5 to -80 °C. Frozen samples were stored at least 24 h at -80 °C and thawed for 5 min at 42 °C before evaluating the biological activity of bacterial cells.

### Cold and osmotic stress treatments

The washed cell pellets were resuspended in the same weight of sucrose solutions of different concentrations (12.5, 25, and 50 % wt) to mimic their exposure to increasing cryoconcentrations. The final osmolarity of bacterial suspensions was (i) isotonic (300 mOsm; 12.5 %), corresponding to the osmolarity of the fermentation medium; (ii) moderately hypertonic (600 mOsm; 25 %), corresponding to the osmolarity of the cryoprotective medium; or (iii) strongly hypertonic (1800 mOsm; 50 %), corresponding to an extreme cryoconcentration, which could be expected in the case of slow freezing rates. Osmolarities were determined using a Roebbling osmometer (Type 13, Löser Messtechnik; Berlin, Germany).

The sucrose-cell suspensions were incubated either at room temperature (25 °C) or at -3 °C by immersion of the cryotubes in a Hyperion calibration liquid bath (AOIP; Ris Orangis, France) filled with silicone oil (Kryo 51, Lauda; Lauda-Königshofen, Germany) for 15 min and 3 h. The subzero temperature value applied for cold stress experiments was chosen from the liquidus curve of sucrose (between the melting point of 25 and 50 % sucrose solutions: -2 and -6 °C, respectively) (Blond et al. 1997). The absence of ice formation during stress exposure was visually verified.

Previous tests were carried out to define the stress time that would ensure complete osmotic dehydration and significant degradation of the biological activity of the sensitive strain, *L. bulgaricus* CFL1 (Passot et al., personal communication; *Cryobiology*, Bristol, UK, 2010). The maximal cell volume reduction (16 %) was observed between 1 and 3 h of incubation under hypertonic conditions at 25 °C. No loss of biological activity was reported after incubation for 3 h under isotonic conditions at 25 °C.

## Biological activity measurement

Two properties were measured to describe the biological activity of *L. bulgaricus*: cell culturability (CFU mL<sup>-1</sup>) and acidifying activity (tm). The measurements were carried out: (i) before and after freezing and (ii) 15 min and 3 h after exposure to cold and osmotic stress treatments. The biological activity of the frozen samples was determined immediately after thawing (5 min at 42 °C).

### Culturability measurement

Bacterial cell concentration was determined using the agar plate count method. Samples were serially diluted in saline water and the appropriate dilutions were inoculated in the bulk of MRS agar (Biokar Diagnostics; Beauvais, France) plates in triplicate. Colonies were enumerated after incubating the plates for 48 h at 42 °C in anaerobic conditions (GENbox anaer, bioMerieux; Marcy l'Etoile, France). Plates containing between 30 and 300 colonies were kept for cell concentration calculation (in CFU mL<sup>-1</sup>).

Culturability loss after freezing or stress treatments (in log (CFU mL<sup>-1</sup>)) was calculated using the following equation (Eq. 1):

$$\text{Culturability loss} = \log \frac{[\text{CFU mL}^{-1}]_{\text{after treatment}}}{[\text{CFU mL}^{-1}]_{\text{reference}}} \quad (1)$$

where [CFU mL<sup>-1</sup>]<sub>reference</sub> refers to cell concentration obtained before freezing or immediately after (15 min) resuspending cells in isotonic sucrose solution at 25 °C, and [CFU mL<sup>-1</sup>]<sub>after treatment</sub> refers to cell concentration determined after freezing, or after a 15-min exposure to moderate and strong sucrose concentrations, or after a 3-h exposure to all osmotic conditions.

### Acidifying activity measurement

The CinAc system (AMS; Frepillon, France) was used to evaluate the acidifying activity of the bacterial suspensions according to Fonseca et al. (2000), with minor modifications. Briefly, 150 mL of skim milk was reconstituted from dry powder at 100 g L<sup>-1</sup> (EPI Ingredients; Ancenis, France), distributed in flasks, sterilized (at 110 °C for 20 min) and prewarmed to 42 °C in a temperature-controlled bath. Following the inoculation of three flasks with 100 µL of the bacterial suspensions, their pH was continuously monitored every 3 min until the end of the acidification. The minimum of the first-order derivative of the acidification curves represents the time required for the bacterial suspension to reach its maximum acidification rate in milk and was used as a discriminating descriptor between experimental conditions (tm, in min).

The higher the tm value was, the longer the latency phase and the lower the acidifying activity were.

The acidifying activity loss (dtm<sub>treatment</sub>, in min) after freezing or stress treatments was quantified as follows (Eq. 2):

$$\text{dtm}_{\text{treatment}} = \text{tm}_{\text{after-treatment}} - \text{tm}_{\text{reference}} \quad (2)$$

where tm<sub>reference</sub> refers to the tm obtained before freezing or immediately after (15 min) resuspending cells in isotonic sucrose solution at 25 °C, and tm<sub>after-treatment</sub> refers to the tm determined after freezing, or after a 15-min exposure to moderate and strong sucrose concentrations or after a 3-h exposure to all osmotic conditions. An increase of the dtm value corresponds to an increased loss of acidification activity during the considered treatment.

### DSC: intracellular glass transition temperature

The intracellular glass transition temperature was determined with a differential scanning calorimeter (Diamond, Perkin Elmer LLC; Norwalk, CT, USA) equipped with a liquid nitrogen cooling accessory (CryoFill; Perkin Elmer) as previously described (Clarke et al. 2013; Fonseca et al. 2016). Cell pellets obtained after the washing steps with Tris–HCl buffer (Fig. 1) were additionally washed with peptone water (1 g L<sup>-1</sup>) prior to DSC scanning. About 20 mg of cell pellets were sealed in an aluminum pan and samples were cooled to –100 °C and then heated to 20 °C at 10 °C min<sup>-1</sup>. Cell pellets obtained from centrifuged cells resuspended in sucrose cryoprotective solution (20 % in saline water) as well as a sample of the sucrose solution (corresponding to the extracellular matrix) were also analyzed for comparison. The glass transition temperatures of the intracellular contents and the sucrose solution, Tg'i and Tg'e (°C), respectively, were calculated from the first derivative of the heat flow recorded during warming (Fonseca et al. 2016).

### FA composition

Membrane fatty acid (FA) composition was determined on cell pellets obtained after the washing steps with Tris–HCl buffer (Fig. 1), according to the method fully described by Gautier et al. (2013) with minor modifications. Briefly, lipid extraction from washed cell pellets was performed by means of accelerated solvent extraction (ASE 350, Dionex; Sunnyvale, CA, USA) using three chloroform/methanol solvent ratios: 2:1, 1:1, and 1:2 (vol) under pressure at 100 °C. FA standards (Larodan; Solna, Sweden) including the cyclic FA cycC19:0 standard as well as freshly extracted phospholipid fatty acyl residues were methylated with trimethylsulfonium hydroxide (TMSH, Sigma-Aldrich; St. Louis, MO, USA) and analyzed by gas chromatography-mass spectrometry (GC-MS) for their identification and



quantification. A Hewlett-Packard 6890 gas chromatograph (GMI; Ramsey, MI, USA) was used. It was equipped with a capillary column packed with 70 % cyanopropyl polysilphenylene-siloxane BPX70 (60 m × 0.25 mm, with a film thickness of 0.25 μm; SGE Analytical Science Pty Ltd.; Victoria, Australia), coupled to a mass spectrometer (5973, Agilent Technologies; Avondale, PA, USA). Results were expressed as FA percentages.

### Steady state fluorescence anisotropy: membrane fluidity measurement

Membrane fluidity of bacterial cells was assessed by measuring the degree of polarization of two fluorescent probes, 1,6-diphenyl-1,3,5-hexatriene (DPH) and 1-[4 (trimethylamino) phenyl]-6-phenyl-1,3,5-hexatriene (TMA-DPH). These probes have strong lipophilic properties that allow them to be inserted into lipid bilayers of models and also complex cellular systems such as Gram-positive bacteria (Tourdot-Maréchal et al. 2000; Tymczyszyn et al. 2005; Chu-Ky et al. 2005; Martos et al. 2007; Passot et al. 2014), Gram-negative bacteria (Chadeau et al. 2012), yeasts (Simonin et al. 2008; Abe and Hiraki 2009), or plant cell endospores (Dubas et al. 2013). Since *L. bulgaricus* does not accumulate lipids in the intracellular compartment, both probes will exclusively locate in the only available cellular lipid reservoir, the cytoplasmic membrane: (i) within the hydrocarbon core for DPH, fully apolar and (ii) at the water/lipid interface for its cationic derivative TMA-DPH (Ben-Yashar and Barenholz 1991; Kaiser and London 1998).

Stock solutions of DPH (0.6 mM, Sigma-Aldrich; St. Louis, MO, USA) and TMA-DPH (2 mM, Molecular Probes; Eugene, OR, USA) were prepared in dimethylsulfoxide (DMSO, Sigma-Aldrich; St. Louis, MO, USA). The method described by Chu-Ky et al. (2005) with minor modifications was applied. Briefly, bacterial samples incubated for 3 h at 25 °C in sucrose solutions of different concentrations were diluted in MES-KOH buffer (50 mM, pH 5.5, Sigma-Aldrich; St. Louis, MO, USA) supplemented with 10 mM glucose to obtain an OD<sub>600 nm</sub> of 0.5. DPH or TMA-DPH from stock solutions was then added to obtain a final probe concentration of 3 or 2 μM, respectively. Staining of bacterial solutions was performed for 3 min in darkness at 25 °C prior to centrifugation (18,500×g for 2 min). The pellets were resuspended in the same volume of the corresponding sucrose solution to maintain osmotic condition during the measurement, and 3 mL was loaded into a stirred quartz cuvette. Fluorescence anisotropy was measured on a Fluorolog-3 spectrofluorometer (Jobin-Yvon Horiba; Longjumeau, France) as previously described (de Sarrau et al. 2013). The excitation wavelength was set at 360 nm and the emission wavelength at 430 nm. Polarizers were located on the

excitation source and on the two photomultiplier tubes to measure anisotropy.

Steady state anisotropy ( $r$ ) was calculated according to the following equation (Eq. 3):

$$r = \frac{I_{vv} - G \times I_{vh}}{I_{vv} + 2G \times I_{vh}} \quad (3)$$

where  $I_{vv}$  and  $I_{vh}$  represent the fluorescence intensity obtained with the vertical and horizontal orientations of the excitation and emission polarizers (e.g.,  $I_{vv}$  is the vertical excitation and vertical emission), and  $G = I_{hv}/I_{hh}$  is a correction factor accounting for the polarization bias in the detection system.

Fluorescence anisotropy is inversely proportional to membrane fluidity: the higher the anisotropy ( $r$ ) is, the more rigid the membrane will be. Anisotropy values were obtained at different sample temperatures ranging from 42 to 0 °C using a Peltier module (LFI-3751, Wavelength electronics; Bozeman, MT, USA). Temperature dynamics were performed from two independent bacterial cultures.

### FTIR spectroscopy: phospholipid organization

Phospholipid organization in biological membranes can be evaluated by Fourier transform infrared (FTIR) spectroscopy by measuring the vibrational energy of specific chemical functional groups relevant to the lipid bilayer. The study was focused on the position of (i) the symmetric  $\text{CH}_2$  stretching vibration band ( $\nu\text{CH}_2 \text{ sym.}$ ) located at approximately  $2850 \text{ cm}^{-1}$  and arising from hydrocarbon chains of phospholipids (Crowe et al. 1989; Gautier et al. 2013; Wolkers and Oldenhof 2015), (ii) the asymmetric  $\text{PO}_2^-$  stretching vibration band ( $\nu\text{PO}_2^- \text{ asym.}$ ) located at approximately  $1220 \text{ cm}^{-1}$  and arising from the phosphate moiety of phospholipid headgroups (Goñi and Arrondo 1986; Linders et al. 1997; Arrondo and Goñi 1998; Lewis and McElhaney 1998; Díaz et al. 2003; Wolkers et al. 2010; Dianawati et al. 2012).

Measurements were carried out on a Nicolet Magna 750 FTIR spectrometer (Thermo Fisher Scientific; Madison, WI, USA) equipped with a mercury/cadmium/telluride (MCT) detector and a variable temperature cell holder (Specac Ltd.; Orpington, Kent, UK), as described by Gautier et al. (2013). A thermocouple inserted as close as possible to the sample made it possible to accurately cool it at a rate of  $2 \text{ °C min}^{-1}$  by continuously pouring liquid nitrogen into the cell holder. The optical bench was continuously purged with dry air (Balston; Haverhill, MA, USA) to remove any spectral contribution from water vapor. Omnic software (version 7.1, Thermo Fisher Scientific; Madison, WI, USA) was used for spectra acquisition: 32 co-added scans were collected every 45 s with a resolution of  $4 \text{ cm}^{-1}$  in the mid-IR region from  $4000$  to  $900 \text{ cm}^{-1}$ .

Bacterial samples incubated for 3 h at 25 °C in sucrose solutions of different concentrations were centrifuged (16,100×g for 5 min), and the cell pellet was tightly sandwiched between two calcium fluoride windows (ISP Optics; Riga, Latvia). The windows were inserted into the cell holder and infrared absorption spectra were recorded during cooling from 50 to −50 °C at 2 °C min<sup>−1</sup>.

Spectra analysis (determination of peak location and lipid phase transition temperature) was performed using ASpIR software (Infrared Spectra Acquisition and Processing, INRA; Thiverval-Grignon, France). To determine specific peak locations from each spectrum, second-order derivatives were calculated, smoothed following a seven-point Savitzky-Golay algorithm, and multiplied by −1. Wavenumbers (or frequencies) of the  $\nu CH_2$  sym. and  $\nu PO_2^-$  asym. peaks were plotted as a function of temperature. The  $\nu CH_2$  sym. plots were fitted with a curve based on an asymmetric sigmoid transition function, and the first-order derivative was calculated. Its maxima was taken as the lipid phase transition following freezing ( $T_s$ ). Ice nucleation was also determined following the upshift of the combination band of OH libration and bending modes of water ( $\nu H_2O$ ) from approx. 2150 to 2220 cm<sup>−1</sup> (Gautier et al. 2013).

## Statistical analyses

Statistical analyses were performed in R 3.2.3 using the R Commander package. Sample means were compared after verifying the normality of their distribution at a 95 % confidence interval. The significance of results was assessed at a 90 % confidence level ( $p$  value <0.1).

## Results

### Freeze resistance, membrane fatty acid composition, and intracellular glass transition temperature of *L. bulgaricus* CFL1 and ATCC 11842 grown in Whey medium

Following freezing and thawing, *L. bulgaricus* ATCC 11842 exhibited no loss of culturability or acidifying activity and thus appeared to be highly resistant to freezing. Conversely, large losses of culturability (−1.4 log units, corresponding to a survival rate of 4 %) and acidifying activity (dtm = 250 min, corresponding to a 4.2 h increase in the acidifying time) were observed for *L. bulgaricus* CFL1 (data reported in Table S1).

Membrane fatty acid compositions of the resistant and sensitive strains are summarized in Table 1. Regardless of the strain, the bacterial membrane was composed of four main fatty acids (FAs), accounting for more than 80 % of the total FA: C14:0, C16:0, C16:1, and C18:1. A total of

**Table 1** Membrane fatty acid composition (relative percentages) of *L. bulgaricus* ATCC 11842 and *L. bulgaricus* CFL1 grown in a Whey-based medium and harvested at the exponential growth phase

Fatty acids (FAs)	ATCC 11842	CFL1
C12:0	3.6 ± 0.7	1.9 ± 0.3
C14:0	7.9 ± 1.7	10.2 ± 1.5
C16:0	27.4 ± 2.7	36.9 ± 4.2
C16:1	21.3 ± 1.9	22.5 ± 1.6
C18:0	6.9 ± 1.1	7.2 ± 2.9
C18:1	25.3 ± 4.0	15.1 ± 4.3
C18:2	2.0 ± 0.6	1.4 ± 0.3
C19:0cyc	3.9 ± 0.9	3.3 ± 0.5
Total SFA <sup>a</sup>	47.5 ± 6.2	57.7 ± 6.0
Total UFA <sup>a, b</sup>	48.6 ± 5.3	39.0 ± 5.7
UFA/SFA	1.04 ± 0.24	0.69 ± 0.16
Long chain FA <sup>a, c</sup>	38.6 ± 3.3	27.7 ± 1.9

Data presented are means of three independent replicates ± standard deviation

SFA saturated FA, UFA unsaturated FA

<sup>a</sup> Total SFA, total UFA and long chain FA include FA from the table plus FA representing less than 1 % of total FA and not shown in the table

<sup>b</sup> Total UFA does not comprise C19:0cyc

<sup>c</sup> Long chain FA comprise FA with 18 carbon atoms or more

14 FAs were detected (low levels of C13:0, C15:0, C17:0, C19:0, C20:0, and C22:0 were detected and quantified; since they represented less than 1 % of the total FA, they were not included in Table 1). These results are in agreement with the membrane FA composition of different strains of *L. bulgaricus* reported in the literature (Veerkamp 1971; Gomez Zavaglia et al. 2000; Tymczyszyn et al. 2005; Gautier et al. 2013).

Both strains exhibited different relative contents of C16:0 and C18:1. The membrane of *L. bulgaricus* ATCC 11842 was richer in C18:1 and thus in unsaturated fatty acid (UFA) than the membrane of *L. bulgaricus* CFL1 ( $p$  value = 0.04). This resulted in different ratios of unsaturated to saturated fatty acids (UFA:SFA): 1.0 for *L. bulgaricus* ATCC 11842 and 0.7 for *L. bulgaricus* CFL1 ( $p$  value = 0.1) and in a higher proportion of long chain FA (number of carbons ≥18) for *L. bulgaricus* ATCC 11842 (38.6 ± 3.3 %) compared to *L. bulgaricus* CFL1 (27.7 ± 1.9 %) ( $p$  value = 0.01).

Furthermore, both strains exhibited slightly different values of intracellular glass transition temperature: −19.2 °C for the washed *L. bulgaricus* ATCC 11842 (±1.2 °C) and −17.4 °C for the washed *L. bulgaricus* CFL1 (±0.9 °C). Adding the cryoprotective solution led to a  $T_g$ 'i decrease in both strains with −27.6 °C (±1.1 °C) and −25.5 (±1.6 °C), respectively. The values reported for *L. bulgaricus* CFL1 were consistent with the recent work of Fonseca et al. (2016).

### Influence of cold and osmotic stress treatments on the biological activity of *L. bulgaricus* (culturability and acidifying activity)

Regardless of the stress condition, *L. bulgaricus* ATCC 11842 exhibited no degradation of culturability and acidifying activity (Fig. 2, data reported in Table S1). Only a minor loss of acidifying activity (less than 30 min) was observed when cells were incubated for 3 h at  $-3\text{ }^{\circ}\text{C}$  under the strongly hypertonic condition (1800 mOsm,  $p$  value = 0.4). Conversely, the biological activity of *L. bulgaricus* CFL1 was strongly affected by osmotic stress treatments. When considering incubation at  $25\text{ }^{\circ}\text{C}$ , loss of culturability progressively increased with increasing osmolarity: no loss at 300 mOsm ( $p$  value = 0.5) and losses of 0.4 and 1.8 log units at 600 and 1800 mOsm, respectively ( $p$  values = 0.1 and 0.001, respectively). No difference in culturability loss was observed in terms of incubation time ( $p$  values  $>0.1$ ). The same incremental trend was

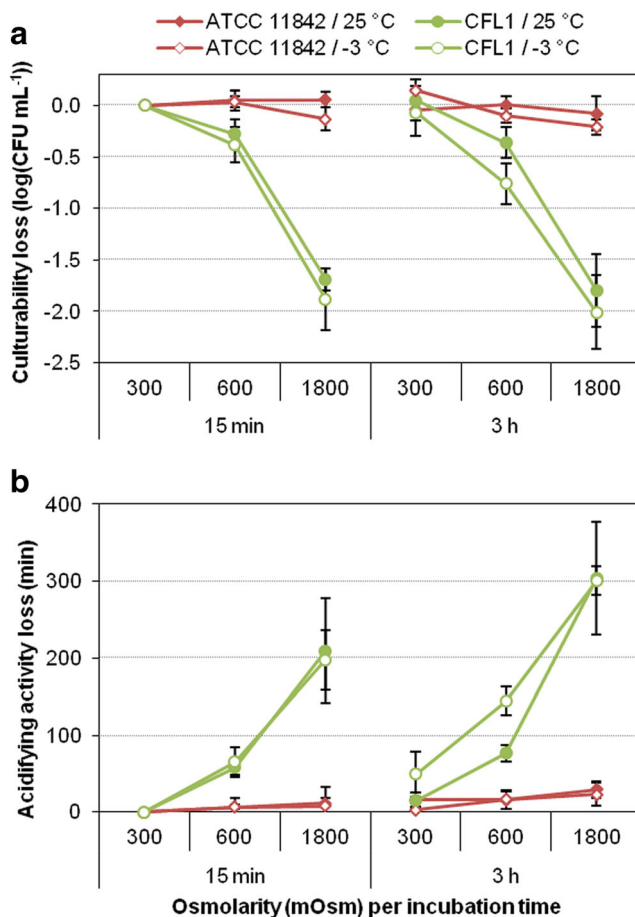


**Fig. 2** Biological activity losses of *L. bulgaricus* ATCC 11842 (in red) and *L. bulgaricus* CFL1 (in green) submitted to an osmotic stress at  $25\text{ }^{\circ}\text{C}$  (filled symbols) or  $-3\text{ }^{\circ}\text{C}$  (open symbols) for 15 min (left side) and 3 h (right side). **a** Loss of culturability (in log (CFU mL<sup>-1</sup>)) and **b** loss of acidifying activity (in min). Values measured after 15 min of exposure at  $25\text{ }^{\circ}\text{C}$  at isotonic condition were considered as the reference condition for the calculation of losses

observed for the loss of acidifying activity but with an impact of the incubation time, especially for the strong hypertonic stress condition (1800 mOsm). Exposure of *L. bulgaricus* CFL1 cells to a mild hypertonic stress (600 mOsm) resulted in an increase of the acidifying time of 85 min, reaching 200 min (or 300 min after 3 h) under strong hypertonic conditions (1800 mOsm) at  $25\text{ }^{\circ}\text{C}$ . An incremental decrease of viability following gradual hyperosmotic stresses with sucrose was also observed by Ragoonanan et al. (2008) on *Geobacter sulfurreducens*.

The sensitivity of *L. bulgaricus* CFL1 to cold stress appeared quite weak. When considering incubation at  $-3\text{ }^{\circ}\text{C}$ , no degradation of the biological activity was observed for the isotonic condition after 3 h of incubation ( $p$  values  $>0.1$ ). The impact of the incubation temperature appeared to be significant only for the moderate hypertonic condition performed for 3 h and resulted in a doubling of the culturability and acidifying activity losses compared to the same treatment performed at  $25\text{ }^{\circ}\text{C}$  ( $p$  values  $<0.05$ ). Degradation of biological activity observed following freezing and thawing of *L. bulgaricus* CFL1 could thus be ascribed to a strong osmotic stress.

### Influence of cold and osmotic stress treatments on membrane fluidity evaluated by fluorescence anisotropy

The fluorescence anisotropy ( $r$ ) of DPH and TMA-DPH probes is negatively related to membrane fluidity (i.e., positively related to membrane rigidity). A schematic drawing was inserted in Fig. 3a to illustrate the commonly reported location of these fluorescent probes within a lipid bilayer.

#### Cold stress

When considering the LAB production process, the fermentation step is followed by chilling from  $42$  to  $5\text{ }^{\circ}\text{C}$  to stop any metabolic activity, and some changes in membrane fluidity are expected. Figure 3a illustrates the evolution of membrane fluidity under isotonic conditions following cooling for both *L. bulgaricus* strains (data reported in Table S2).

Regardless of the strain and probe, decreasing temperatures resulted in an increase in fluorescence anisotropy and, as a result, in membrane rigidification ( $p$  values  $<0.02$  for DPH and  $p$  values  $<0.07$  for TMA-DPH). Furthermore, this rigidification appeared to be more pronounced at the center of the membrane (DPH) than at the periphery (TMA-DPH), with an increase of anisotropy of approximately 100 and 30 %, respectively.

When comparing both strains, some differences can also be observed in membrane fluidity. At  $42\text{ }^{\circ}\text{C}$  (LAB growth temperature), membrane fluidity at the center was similar for both strains ( $p$  value = 0.4), whereas the external membrane surface tended to be more rigid in *L. bulgaricus* ATCC 11842 than in *L. bulgaricus* CFL1 ( $p$  value = 0.2). At  $0\text{ }^{\circ}\text{C}$  (close to the



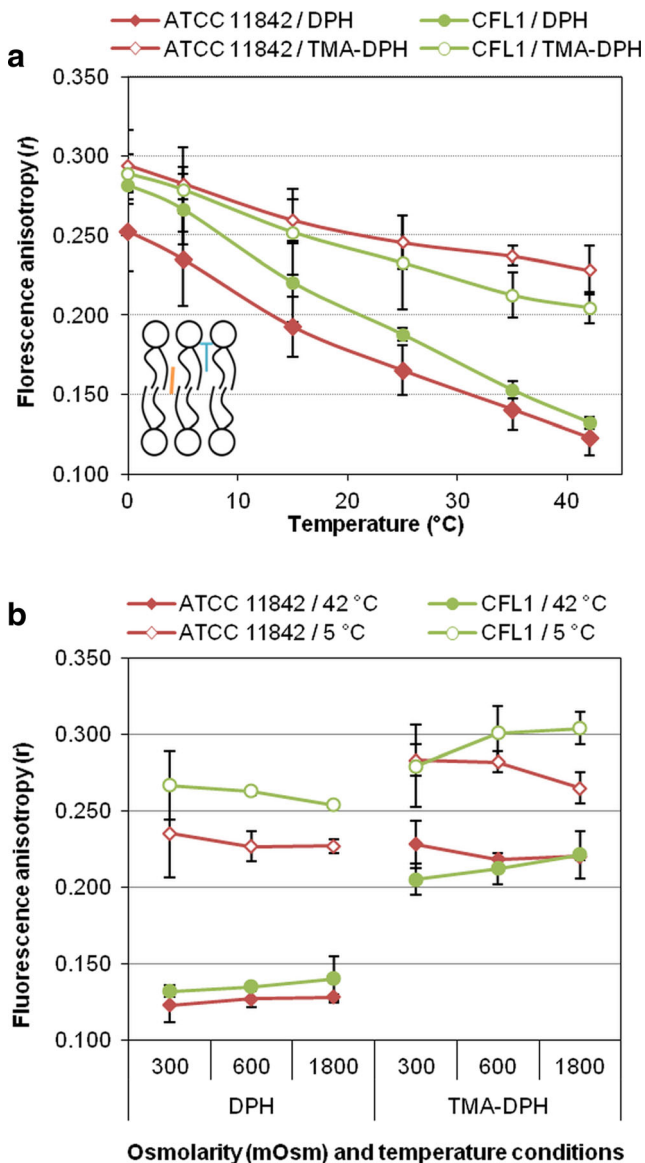


**Fig. 3** Membrane fluorescence anisotropy (*r*) of *L. bulgaricus* ATCC 11842 (in red) and *L. bulgaricus* CFL1 (in green) **a** upon cooling under isotonic conditions and **b** as a function of osmotic strength for selected temperatures (42 and 5 °C). Filled symbols represent **a** DPH anisotropy or **b** 42 °C and open symbols represent **a** TMA-DPH anisotropy or **b** 5 °C. The diagram inserted in **a** illustrates the position of the DPH (orange bar) and the TMA-DPH probes (blue “T”) within the lipid bilayer

formation of ice), the membrane core of *L. bulgaricus* ATCC 11842 became more fluid than *L. bulgaricus* CFL1, but the external surface of both strains reached similar rigidity levels. Furthermore, the membrane core and external surface of *L. bulgaricus* CFL1 were characterized by similar anisotropy values at 0 °C ( $0.285 \pm 0.011$ , *p* value = 0.6).

#### Osmotic stress

Figure 3b illustrates the influence of osmotic stress on membrane fluidity of both strains for two values of temperature

representative of our experimental approach: 42 °C for the growth temperature and 5 °C for the temperature applied during harvesting and formulation steps (data reported in Table S2). Exposing cells to hypertonic conditions did not seem to affect membrane core fluidity (DPH). A slight change in membrane fluidity was detected at 5 °C for the external membrane surface (TMA-DPH) but was not significant; increasing sucrose concentrations tended to increase anisotropy values (i.e., increased membrane rigidity) for *L. bulgaricus* CFL1 (*p* value = 0.3) and to decrease anisotropy values (i.e., increased membrane fluidity) for *L. bulgaricus* ATCC 11842 (*p* value = 0.2).

#### Influence of cold and osmotic stress treatments on membrane phospholipid organization evaluated by FTIR spectroscopy

FTIR spectroscopy was used to characterize changes in membrane phospholipid organization by tracking the vibration band position of two specific chemical groups during freezing: (i) the  $\nu\text{CH}_2$  sym. arising from phospholipid acyl chains (i.e., related to the central part of the bilayer) and (ii) the  $\nu\text{PO}_2^-$  asym. involving phosphate groups of the external surface of the bilayer.

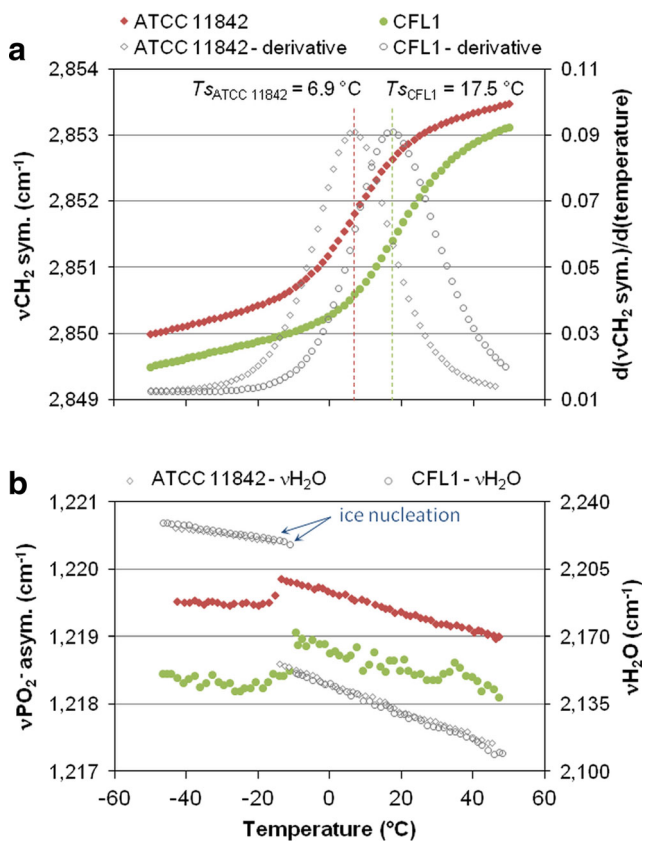
#### Cold stress

Figure 4a, b displays the evolution of the band position of  $\nu\text{CH}_2$  sym. and  $\nu\text{PO}_2^-$  asym. following cooling from 50 to  $-50$  °C for both strains under isotonic conditions, respectively. In Fig. 4b, the  $\nu\text{H}_2\text{O}$  was also plotted with temperature to identify the ice nucleation event (data reported in Table S2). Ice formation was visible during cooling as an abrupt increase in wavenumber, which occurred spontaneously at around  $-10$  °C.

When considering the  $\nu\text{CH}_2$  sym. (Fig. 4a), decreasing temperatures resulted in a shift of the band position to lower wavenumber values. This is known to reflect membrane lipid phase transition from a relatively disordered fluid lipid state, referred to as the liquid crystalline phase, to an ordered rigid lipid state, referred to as the gel phase (Crowe et al. 1989; Wolkers and Oldenhof 2015).

The first derivative of the  $\nu\text{CH}_2$  sym. vs. the temperature curve was plotted to determine the lipid phase transition during freezing ( $T_s$ ), reported in Fig. 4a. *L. bulgaricus* ATCC 11842 exhibited a significantly lower  $T_s$  value ( $6.9 \pm 1.3$  °C) than *L. bulgaricus* CFL1 ( $17.5 \pm 1.8$  °C) (*p* value = 0.001). In addition, *L. bulgaricus* ATCC 11842 cells showed higher  $\nu\text{CH}_2$  sym. wavenumbers regardless of the temperature, and especially in the frozen state (*p* value = 0.01 at  $-48$  °C). This suggests that membrane of *L. bulgaricus* ATCC 11842 exhibited less ordered lipid acyl chains than membrane of *L. bulgaricus* CFL1.





**Fig. 4** Peak position of the **a** symmetric  $\text{CH}_2$  stretching ( $\nu\text{CH}_2\ \text{sym.}$ ) and **b** asymmetric  $\text{PO}_2^-$  stretching ( $\nu\text{PO}_2^-\ \text{asym.}$ ) vibration bands arising from *L. bulgaricus* ATCC 11842 (in red) and *L. bulgaricus* CFL1 (in green) upon cooling under isotonic conditions. In **a**, lipid solidification temperatures ( $T_s$ ) are highlighted by the maximum of the first derivatives of the curves (open symbols). In **b**, ice nucleation corresponds to the shift in the  $\text{H}_2\text{O}$  libration and bending band ( $\nu\text{H}_2\text{O}$ , open symbols) from approx. 2150 to 2220  $\text{cm}^{-1}$ . For the sake of clarity, standard deviations were not included

When considering  $\text{PO}_2^-$  groups (Fig. 4b), decreasing temperature resulted in a linear elevation of the band position until ice nucleation occurred, at which point an abrupt wavenumber downshift was observed. The peak position remained at quite constant values with further temperature decrease. Regardless of the temperature, *L. bulgaricus* ATCC 11842 cells exhibited higher  $\text{PO}_2^-$  wavenumber positions than *L. bulgaricus* CFL1 cells ( $p$  values  $<0.07$ ). Moreover, the downshift observed upon ice nucleation was less extensive for strain ATCC 11842 compared to strain CFL1.

Since the thermotropic behavior of the  $\nu\text{PO}_2^-\ \text{asym.}$  was directly affected by ice nucleation, the vibration of  $\text{PO}_2^-$  moieties could be attributed to bacterial macromolecules that are directly in contact with the extracellular medium, such as the external leaflet of the phospholipid bilayer and not nucleic acids or intracellular phosphorylated molecules (Dianawati et al. 2012).

Osmotic stress

Applying osmotic stress to cells did not modify the lipid phase transition temperature ( $T_s$ ) for *L. bulgaricus* ATCC 11842 ( $p$ -values  $>0.2$ ) but resulted in a 4  $^\circ\text{C}$  decrease of the  $T_s$  value for *L. bulgaricus* CFL1 under strong hypertonic conditions ( $13.6\ ^\circ\text{C} \pm 2.2\ ^\circ\text{C}$ ) ( $p$  value = 0.08). Figure 5a, b illustrates the influence of osmotic stress on the position of the  $\nu\text{CH}_2\ \text{sym.}$  and  $\nu\text{PO}_2^-\ \text{asym.}$  for selected values of temperatures, respectively (data reported in Table S2). The value of  $-48\ ^\circ\text{C}$  corresponds to the extracellular glass transition temperature ( $T_g^e$ ).

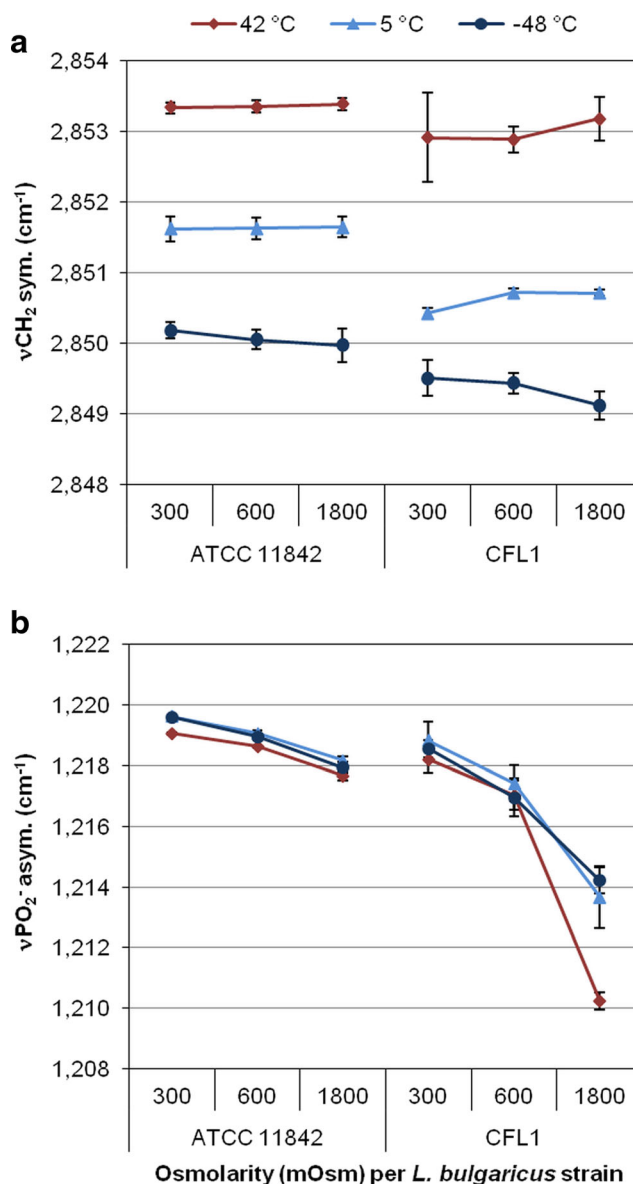


**Fig. 5** Peak position of the **a** symmetric  $\text{CH}_2$  stretching ( $\nu\text{CH}_2\ \text{sym.}$ ) and **b** asymmetric  $\text{PO}_2^-$  stretching ( $\nu\text{PO}_2^-\ \text{asym.}$ ) vibration bands arising from *L. bulgaricus* ATCC 11842 (left) and *L. bulgaricus* CFL1 (right) as a function of osmotic strength for selected temperatures

When considering *L. bulgaricus* ATCC 11842 (Fig. 5a), no change in the peak position of the  $\nu\text{CH}_2$  sym. (related to the membrane core; Fig. 5a) with osmolarity was observed, regardless of the temperature values ( $p$  values  $>0.2$ ) (consistent with the DPH fluidity invariability with osmolarity increase in Fig. 2b). However, for the  $\nu\text{PO}_2^-$  asym., a slight shift to lower wavenumbers when increasing osmolarity was observed. Consequently, for strain ATCC 11842, osmotic stress would not affect membrane core conformational order. It would, however, affect the conformational order of phospholipid headgroups but only to a slight extent.

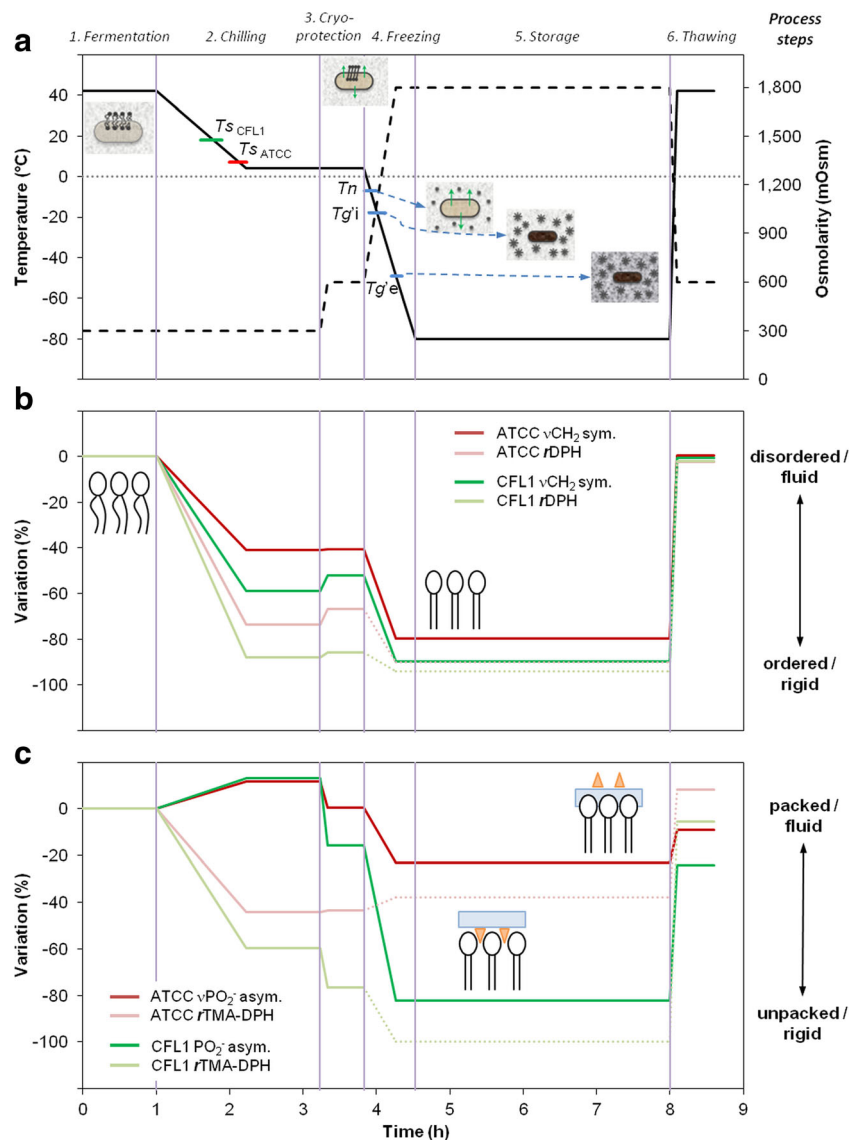
When considering *L. bulgaricus* CFL1, cell exposure to hypertonic conditions extensively modified the lipid membrane organization (Fig. 5a, b). At 5 °C, the  $\nu\text{CH}_2$  sym. slightly upshifted with increasing osmolarity, denoting a higher conformational disorder of the lipid acyl chains. However, the shift occurred to a lower wavenumber in the frozen state,

indicative of a conformational ordering of the lipid acyl chains ( $p$  values  $<0.2$ ). The  $\nu\text{PO}_2^-$  asym. also shifted to lower wavenumbers in *L. bulgaricus* CFL1 but to a greater extent than *L. bulgaricus* ATCC 11842, especially under strong hypertonic conditions at 42 °C ( $p$  values  $<0.03$ ). The external surface of the membrane of *L. bulgaricus* CFL1 was therefore extensively affected by hypertonic stress.

## Discussion

Even if the physical events that occur during the freezing of cells are well-known at this time, maintaining their biological activity still remains a challenge, especially for lactic acid bacteria (LAB). Freezing can be considered as a combination of different stresses applied to bacterial cells: exposure to cold temperatures, ice formation, and high concentrations of

**Fig. 6** **a** Schematic overview of the main transitions (lipid:  $T_s$ ; water:  $T_n$ ; glass:  $T_g^i$  and  $T_g^e$ ) occurring during cryopreservation of *L. bulgaricus* as a function of temperature (solid black line, °C) and osmolarity (dashed black line, mOsm), representative of six successive steps of the process. Membrane fluidity and organization variations of **b** the core and **c** external surface of the lipid bilayer are represented as percentage changes relative to the values corresponding to the end of fermentation: **b** DPH and **c** TMA-DPH anisotropy of *L. bulgaricus* ATCC 11842 (in light red) and *L. bulgaricus* CFL1 (in light green); **b** symmetric  $\text{CH}_2$  stretching ( $\nu\text{CH}_2$  sym.) and **c** asymmetric  $\text{PO}_2^-$  stretching ( $\nu\text{PO}_2^-$  asym.) of *L. bulgaricus* ATCC 11842 (in red) and *L. bulgaricus* CFL1 (in green). Cell diagrams in **a** were adapted from Fonseca et al. (2016). Diagrams in **c** illustrate the putative interaction of sucrose (orange triangles) and water (blue boxes) with membrane phospholipids of *L. bulgaricus* ATCC 11842 (top right; preferential exclusion) and CFL1 (bottom; preferential interaction). *L. bulgaricus* ATCC 11842 was abbreviated ATCC for the sake of clarity



solutes. When applying slow cooling rates, cells are densely packed in the cryoconcentrated matrix, sharply reducing the direct contact between ice crystals and cells (Fonseca et al. 2006). The present work thus focused on the study of the individual contribution of cold and osmotic stress on the biophysical properties of bacterial membranes in relationship to the degradation of biological activity for two strains of LAB with different freeze resistances. To our knowledge, only two studies have applied a similar approach to the Gram-negative bacterium *Escherichia coli* (Moussa et al. 2008; Simonin et al. 2015). The authors reported that maintaining cell suspensions in the presence of glycerol in a supercooled state for several hours ( $-20\text{ }^{\circ}\text{C}$  without the formation of ice) was more damaging for cell viability and membranes than were cell exposure to high concentrations of glycerol. In the case of *L. bulgaricus* CFL1, a Gram-positive bacterium, the detrimental effect of exposure to cold temperatures appeared quite limited and was detected only after 3 h at moderate hyperosmotic conditions. Conversely, high losses of culturability and acidifying activity were observed after only 15 min of exposure to strong hyperosmotic conditions, making osmotic stress the most cell-damaging event following freezing. Exposing *L. bulgaricus* cells to osmotic stress (i.e., to high concentrations of sucrose, a non-permeating molecule) induces water transport from the intracellular medium of the cell to the extracellular medium, which, in turn, will result in cell dehydration and cell volume contraction. Depending on the flexibility of the membrane, cell volume reduction could easily occur (*L. bulgaricus* ATCC 11842, the resistant strain) or be associated with considerable mechanical constraints (*L. bulgaricus* CFL1, the sensitive strain), possibly leading to membrane leakage.

The analysis of membrane fatty acid (FA) composition, lipid phase transition ( $T_s$ ), and fluidity determined by fluorescence anisotropy showed that both strains exhibited different cytoplasmic membrane properties. The membrane of the resistant strain (*L. bulgaricus* ATCC 11842) was characterized by a higher content of UFA (49 %), a lower lipid phase transition following cooling ( $T_s = 6.9\text{ }^{\circ}\text{C}$ ), and higher membrane fluidity at the center and external surface at  $0\text{ }^{\circ}\text{C}$  than the membrane of the sensitive one (*L. bulgaricus* CFL1: UFA = 39 %;  $T_s = 17.5\text{ }^{\circ}\text{C}$ ). The relationship between membrane composition, in particular the presence of unsaturated fatty acids, and the improvement of freeze resistance of LAB is well established in literature (Beal et al. 2001; Streit et al. 2011; Gautier et al. 2013). The UFA/SFA ratio is sometimes used for evaluating membrane fluidity (Álvarez-Ordóñez et al. 2008). The higher the UFA/SFA ratio, the more fluid the membrane and the higher the freeze resistance are. When considering the growth temperature ( $42\text{ }^{\circ}\text{C}$ ), the membranes of both strains exhibited similar fluidity values, despite different UFA/SFA ratios. The higher proportion of long chain FA within the membrane of *L. bulgaricus* ATCC 11842 (38.6 %)

compared to CFL1 (27.7 %) could compensate for the fluidifying effect from unsaturations (Denich et al. 2003). Membrane fluidity could therefore be correlated with a combination of different fatty acid structures, including unsaturations and chain length. However, membrane fluidity is also dependent on temperature and it is thus important to determine its evolution with a temperature profile relevant to the process studied. In previous works we showed that by modifying growth culture conditions the freezing resistance of *L. bulgaricus* CFL1 could be improved (Gautier et al. 2013; Passot et al. 2014). By growing cells in MRS broth, the membrane became rich in cyclic and unsaturated fatty acids, which, in turn, was associated with a low lipid phase transition temperature ( $T_s = -8\text{ }^{\circ}\text{C}$ ) and high membrane fluidity at subzero temperatures when approaching ice nucleation. Freezing resistance of *L. bulgaricus* ATCC 11842 could thus be ascribed to a cytoplasmic membrane in a more fluid and flexible state around ice nucleation, which facilitates water efflux from the intracellular medium and cell shrinkage following cryoconcentration. However, in these two previous studies, membrane biophysical properties were characterized following cooling in the absence of any protective agent. In the present work, the osmotic stress is expressly addressed by investigating the change of membrane properties as a function of the two main environmental changes induced by freezing: low temperature and high osmotic condition.

Bacterial membrane organization was characterized using two complementary approaches: fluorescence anisotropy providing a direct measurement of membrane fluidity and vibrational spectroscopy affording molecular insight on lipid bilayer organization. Data were obtained at two different locations within the membrane: (i) at the lipid acyl chains region by the anisotropy of DPH probe or the position of the symmetric  $\text{CH}_2$  stretching band at approximately  $2850\text{ cm}^{-1}$  and (ii) at the polar headgroup region by the anisotropy of TMA-DPH probe or the position of the asymmetric  $\text{PO}_2^-$  stretching band at approximately  $1219\text{ cm}^{-1}$ . The frequency (or wavenumber) of the  $\nu\text{CH}_2\text{ sym}$  peak is often reported as an indirect way for evaluating membrane fluidity by providing information related to the degree of conformational order or disorder of the lipid acyl chains (Beney and Gervais 2001; Alvarez-Ordóñez et al. 2011). However, in molecular terms, a frequency shift has to be interpreted as a change of the force constant of the bond considered in the FTIR spectrum. A shift to higher frequencies is related to an increase in the force constant, i.e., a strengthening of the C–H, or P=O bonds in our case (Disalvo et al. 2013). Considering the  $\nu\text{CH}_2\text{ sym}$  vibration, decreasing the temperature results in a shift to lower frequencies. The transition of acyl chain rotamers from *gauche* to all-*trans* conformation following cooling leads to a straightening and packing of acyl chains (Borchman et al. 1991). This decrease in interchain distances reinforces interchain interactions thereby weakening the C–H bond. When

considering the  $\nu PO_2^-$  *asym.* vibration, a shift to lower frequencies and thus a weakening of the P=O bonds could be related to the interaction of the phospholipid headgroups with other groups of the surrounding medium. The band position of the  $\nu PO_2^-$  *asym.* was frequently used to indicate the phospholipid headgroup hydrogen bonding state (Goñi and Arrondo 1986; Arrondo and Goñi 1998; Lewis and McElhaneý 1998). The involvement of phosphate groups in hydrogen bonding with the environment decreases the frequency of this vibration. Conversely, a shift to higher frequencies reveals a decrease in hydrogen bonding and has been linked to an increased phosphate headgroups packing (Díaz et al. 2003; Frías et al. 2006).

To discuss the results and their relevance for explaining freeze resistance, a dynamic representation of the behavior of bacterial cells and membrane properties following environmental changes induced by freezing is proposed in Fig. 6. Figure 6a illustrates the evolution of sample temperature and osmolarity from the end of cell culture to the thawing of frozen samples of *L. bulgaricus* ATCC 11842 and CFL1, according to the experimental approach applied in this study (Fig. 1). The main physical events occurring in the samples (lipid phase transition ( $T_s$ ), nucleation ( $T_n$ ), and glass transition ( $Tg'i$  and  $Tg'e$ ) temperatures), as well as schematic drawings of the physical state of the cells are also reported in Fig. 6a. After fermentation (step 1), membranes of *L. bulgaricus* are in a fluid crystalline phase and change to a gel state following chilling at 5 °C (step 2). The addition of the cryoprotective agent (sucrose, step 3) results in an increase of osmolarity (600 mOsm) which in turn leads to water transport from the intracellular medium and cell dehydration. At approximately -10 °C ( $T_n$ ), ice nucleation occurs and the formation of ice crystals in the extracellular medium begins (step 4). This is associated with increasing osmolarity and further cell dehydration due to the cryoconcentration of the extracellular matrix. Cell dehydration terminates at  $Tg'i$  (i.e., in *L. bulgaricus* CFL1 first, and then in *L. bulgaricus* ATCC 11842) with vitrification of the intracellular matrix, and osmolarity reaches its maximal value when vitrification of the extracellular matrix occurs ( $Tg'e$ ). The temperature continues to decrease until it reaches -80 °C.

The evolution of the properties of the central part of membrane is represented in Fig. 6b by plotting the variation of DPH anisotropy values and  $\nu CH_2$  *sym.* positions with time. The variation of TMA-DPH anisotropy values and the  $\nu PO_2^-$  *asym.* position are used to describe the evolution of the external surface part of the membrane and are plotted in Fig. 6b. The evolution of membrane properties was expressed as percentage changes relative to the values corresponding to the end of fermentation (42 °C, 300 mOsm; step 1). Negative variations of anisotropy indicate a decrease of membrane fluidity (i.e., membrane rigidification). Fluorescence anisotropy measurements were technically limited to 0 °C. The steps of

the process performed below this temperature were therefore reconstructed using the lowest measurable membrane fluidity values, represented as dotted lines in Fig. 6b, c. Negative variations of  $\nu CH_2$  *sym.* and  $\nu PO_2^-$  *asym.* indicate a shift to lower frequencies, which in turn describe lipid acyl chain packing and involvement of phospholipid headgroups in hydrogen bonding, respectively. The organization of the lipid acyl chains of phospholipids is strongly affected by temperature. Following cooling, the acyl chains become densely packed and ordered, which is related to an increase of membrane rigidity measured by the fluorescence probes (DPH and TMA-DPH). A moderate difference exists between both strains. Following chilling to 5 °C (step 2), membrane lipid phase transition is almost completed for *L. bulgaricus* CFL1 ( $T_s = 17.5$  °C and the variation reaches 60 %) and is still in progress in *L. bulgaricus* ATCC 11842 ( $T_s = 6.9$  °C and the variation reaches 40 %). Osmotic stress, the most damaging stress on *L. bulgaricus*, has minor impact on lipid acyl chains but highly altered the organization of the polar headgroups, in particular for the freeze-sensitive strain CFL1. The variation of the  $\nu PO_2^-$  *asym.* band position reached 80 % in *L. bulgaricus* CFL1 (corresponding to a downshift of 8.0  $cm^{-1}$ ) vs. 20 % in *L. bulgaricus* ATCC 11842.

The band position of the  $\nu PO_2^-$  *asym.* has frequently been used to estimate the protective effect of various solutes toward drying (Linders et al. 1997), but few studies have linked it to freezing or cold and osmotic stresses. Adding sucrose to dimyristoyl-phosphatidylcholine (DMPC) multilamellar liposome solutions under hydrated conditions resulted in a depression of the band position of 17  $cm^{-1}$  (Díaz et al. 2003). The authors deduced that strong interactions existed between the solutes they used and the phosphate headgroups, leading to a displacement of water molecules in hydrated conditions. Hinchá and Crowe (1998) reported that membrane leakages observed following freezing in the presence of sugars could be due to hydrogen bonding of sucrose and other sugars to phospholipid headgroups. The intense wavenumber downshift observed for *L. bulgaricus* CFL1 (the sensitive strain) under strong hypertonic conditions (8.0  $cm^{-1}$ ), associated with a degradation of its biological activity, could therefore be the result of a displacement of water molecules weakly bound to phospholipid headgroups by sucrose. The direct interactions between sucrose and phospholipid headgroups could thus result in an alteration of membrane integrity. Conversely, this band position was barely affected by osmolarity in *L. bulgaricus* ATCC 11842 (1.5  $cm^{-1}$  downshift), suggesting less direct interactions between its membrane and the sugar. Moreover, the membrane acyl chain ordering degree and lipid phase transition ( $T_s$ ) were equal under hypertonic and isotonic conditions. This strongly suggests that sucrose did not alter the membrane core structure of *L. bulgaricus* ATCC 11842. According to Wolkers et al. (2010), the maintenance of the hydrogen bonding level to phospholipid headgroups



associated with that of hydrocarbon chain disordering level is the sign of preferential exclusion of the solute from the bilayer hydration shell. Preferential exclusion could thus be the preservation mechanism exerted by sucrose on *L. bulgaricus* ATCC 11842. These putative interaction mechanisms between sucrose and the membrane phospholipids of *L. bulgaricus* CFL1 and ATCC 11842 are schematically illustrated on Fig. 6c.

In this work, freezing was considered as a combination of two distinct stresses by exposing cells to cold and/or osmotic treatments. For the first time, it was evidenced that the organization of the headgroups of membrane phospholipids and in particular its modification with osmotic stress, plays a key role in cryopreservation of lactic acid bacteria. Furthermore, monitoring the position of the asymmetric stretching vibration of  $\text{PO}_2^-$  groups with temperature appeared to be a simple and relevant tool to select the optimal cryoprotective agent or fermentation conditions making it possible to obtain freeze-resistant cells.

**Acknowledgments** This work was supported by the National Institute for Agronomic Research (INRA) and the French National Research Agency (ANR) under the Investing in the Future Program, Grant no. ANR-10-IDEX-0003-02. We are grateful to our colleague Caroline Pénicaud for providing help with fatty acid extraction and analysis, to Hervé Guillemain for ASPIR software adaptation and to Jiawei Xu for the experimental help with assessments of biological activities.

#### Compliance with ethical standards

**Conflict of interest** The authors declare that they have no conflict of interest.

**Ethical approval** This article does not contain any studies with human participants or animals performed by any of the authors.

## References

- Abe F, Hiraki T (2009) Mechanistic role of ergosterol in membrane rigidity and cycloheximide resistance in *Saccharomyces cerevisiae*. *Biochim Biophys Acta BBA-Biomembr* 1788:743–752. doi:10.1016/j.bbame.2008.12.002
- Álvarez-Ordóñez A, Fernández A, López M, Arenas R, Bernardo A (2008) Modifications in membrane fatty acid composition of *Salmonella typhimurium* in response to growth conditions and their effect on heat resistance. *Int J Food Microbiol* 123:212–219. doi:10.1016/j.ijfoodmicro.2008.01.015
- Álvarez-Ordóñez A, Mouwen DJM, López M, Prieto M (2011) Fourier transform infrared spectroscopy as a tool to characterize molecular composition and stress response in foodborne pathogenic bacteria. *J Microbiol Methods* 84:369–378. doi:10.1016/j.mimet.2011.01.009
- Arrondo JL, Goñi FM (1998) Infrared studies of protein-induced perturbation of lipids in lipoproteins and membranes. *Chem Phys Lipids* 96:53–68
- Beal C, Fonseca F, Corrieu G (2001) Resistance to freezing and frozen storage of *Streptococcus thermophilus* is related to membrane fatty acid composition. *J Dairy Sci* 84:2347–2356. doi:10.3168/jds.S0022-0302(01)74683-8
- Beney L, Gervais P (2001) Influence of the fluidity of the membrane on the response of microorganisms to environmental stresses. *Appl Microbiol Biotechnol* 57:34–42. doi:10.1007/s002530100754
- Ben-Yashar V, Barenholz Y (1991) Characterization of the core and surface of human plasma lipoproteins. A study based on the use of five fluorophores. *Chem Phys Lipids* 60:1–14. doi:10.1016/0009-3084(91)90009-Z
- Blond G, Simatos D, Catté M, Dussap CG, Gros JB (1997) Modeling of the water-sucrose state diagram below 0 °C. *Carbohydr Res* 298:139–145. doi:10.1016/S0008-6215(96)00313-8
- Borchman D, Yappert MC, Herrell P (1991) Structural characterization of human lens membrane lipid by infrared spectroscopy. *Invest Ophthalmol Vis Sci* 32:2404–2416
- Chadeau E, Dumas E, Adt I, Degraeve P, Noël C, Girodet C, Oulhal N (2012) Assessment of the mode of action of polyhexamethylene biguanide against *Listeria innocua* by Fourier transformed infrared spectroscopy and fluorescence anisotropy analysis. *Can J Microbiol* 58:1353–1361. doi:10.1139/w2012-113
- Chu-Ky S, Tourdot-Marechal R, Marechal P-A, Guzzo J (2005) Combined cold, acid, ethanol shocks in *Oenococcus oeni*: effects on membrane fluidity and cell viability. *Biochim Biophys Acta BBA - Biomembr* 1717:118–124. doi:10.1016/j.bbame.2005.09.015
- Clarke A, Morris GJ, Fonseca F, Murray BJ, Acton E, Price HC (2013) A low temperature limit for life on earth. *PLoS One* 8:e66207. doi:10.1371/journal.pone.0066207
- Crowe JH, Crowe LM, Carpenter JF, Rudolph AS, Wistrom CA, Spargo BJ, Anchordoguy TJ (1988) Interactions of sugars with membranes. *Biochim Biophys Acta BBA-Rev Biomembr* 947:367–384. doi:10.1016/0304-4157(88)90015-9
- Crowe JH, Hoekstra FA, Crowe LM, Anchordoguy TJ, Drobnis E (1989) Lipid phase transitions measured in intact cells with Fourier transform infrared spectroscopy. *Cryobiology* 26:76–84. doi:10.1016/0011-2240(89)90035-7
- Crowe JH, Carpenter JF, Crowe LM, Anchordoguy TJ (1990) Are freezing and dehydration similar stress vectors? A comparison of modes of interaction of stabilizing solutes with biomolecules. *Cryobiology* 27:219–231. doi:10.1016/0011-2240(90)90023-W
- de Sarrau B, Clavel T, Zwickel N, Despres J, Dupont S, Beney L, Tourdot-Maréchal R, Nguyen-the C (2013) Unsaturated fatty acids from food and in the growth medium improve growth of *Bacillus cereus* under cold and anaerobic conditions. *Food Microbiol* 36:113–122. doi:10.1016/j.fm.2013.04.008
- Denich TJ, Beaudette LA, Lee H, Trevors JT (2003) Effect of selected environmental and physico-chemical factors on bacterial cytoplasmic membranes. *J Microbiol Methods* 52:149–182. doi:10.1016/S0167-7012(02)00155-0
- Dianawati D, Mishra V, Shah NP (2012) Role of calcium alginate and mannitol in protecting *Bifidobacterium*. *Appl Environ Microbiol* 78:6914–6921. doi:10.1128/AEM.01724-12
- Díaz SB, Biondi de Lopez AC, Disalvo EA (2003) Dehydration of carbonyls and phosphates of phosphatidylcholines determines the lytic action of lysoderivatives. *Chem Phys Lipids* 122:153–157. doi:10.1016/S0009-3084(02)00186-X
- Disalvo EA, Bouchet AM, Frias MA (2013) Connected and isolated  $\text{CH}_2$  populations in acyl chains and its relation to pockets of confined water in lipid membranes as observed by FTIR spectrometry. *Biochim Biophys Acta BBA-Biomembr* 1828:1683–1689. doi:10.1016/j.bbame.2013.02.007
- Dubas E, Janowiak F, Krzewska M, Hura T, Żur I (2013) Endogenous ABA concentration and cytoplasmic membrane fluidity in microspores of oilseed rape (*Brassica napus* L.) genotypes differing in

- responsiveness to androgenesis induction. *Plant Cell Rep* 32:1465–1475. doi:10.1007/s00299-013-1458-6
- Fernández Murga ML, Cabrera GM, De Valdez GF, Disalvo A, Seldes AM (2000) Influence of growth temperature on cryotolerance and lipid composition of *Lactobacillus acidophilus*. *J Appl Microbiol* 88:342–348. doi:10.1046/j.1365-2672.2000.00967.x
- Fernández Murga ML, de Valdez GF, Disalvo EA (2001) Effect of lipid composition on the stability of cellular membranes during freeze-thawing of *Lactobacillus acidophilus* grown at different temperatures. *Arch Biochem Biophys* 388:179–184. doi:10.1006/abbi.2001.2274
- Fonseca F, Béal C, Corrieu G (2000) Method of quantifying the loss of acidification activity of lactic acid starters during freezing and frozen storage. *J Dairy Res* 67:83–90
- Fonseca F, Béal C, Corrieu G (2001) Operating conditions that affect the resistance of lactic acid bacteria to freezing and frozen storage. *Cryobiology* 43:189–198. doi:10.1006/cryo.2001.2343
- Fonseca F, Marin M, Morris GJ (2006) Stabilization of frozen *Lactobacillus delbrueckii* subsp. *bulgaricus* in glycerol suspensions: freezing kinetics and storage temperature effects. *Appl Environ Microbiol* 72:6474–6482. doi:10.1128/AEM.00998-06
- Fonseca F, Meneghel J, Cenard S, Passot S, Morris GJ (2016) Determination of intracellular vitrification temperatures for unicellular micro organisms under conditions relevant for cryopreservation. *PLoS One* 11:e0152939. doi:10.1371/journal.pone.0152939
- Frias MA, Diaz SB, Ale NM, Ben Altabef A, Disalvo EA (2006) FTIR analysis of the interaction of arbutin with dimyristoyl phosphatidylcholine in anhydrous and hydrated states. *Biochim Biophys Acta BBA - Biomembr* 1758:1823–1829. doi:10.1016/j.bbamem.2006.06.024
- Gautier J, Passot S, Pénicaud C, Guillemin H, Cenard S, Lieben P, Fonseca F (2013) A low membrane lipid phase transition temperature is associated with a high cryotolerance of *Lactobacillus delbrueckii* subspecies *bulgaricus* CFL1. *J Dairy Sci* 96:5591–5602. doi:10.3168/jds.2013-6802
- Gomez Zavaglia A, Disalvo EA, De Antoni GL (2000) Fatty acid composition and freeze-thaw resistance in lactobacilli. *J Dairy Res* 67:241–247
- Goñi FM, Arrondo JLR (1986) A study of phospholipid phosphate groups in model membranes by Fourier transform infrared spectroscopy. *Faraday Discuss Chem Soc* 81:117–126. doi:10.1039/DC9868100117
- Hincha DK, Crowe JH (1998) Trehalose increases freeze-thaw damage in liposomes containing chloroplast glycolipids. *Cryobiology* 36:245–249. doi:10.1006/cryo.1998.2074
- Hubálek Z (2003) Protectants used in the cryopreservation of microorganisms. *Cryobiology* 46:205–229. doi:10.1016/S0011-2240(03)00046-4
- Kaiser RD, London E (1998) Location of diphenylhexatriene (DPH) and its derivatives within membranes: comparison of different fluorescence quenching analyses of membrane depth. *Biochemistry (Mosc)* 37:8180–8190. doi:10.1021/bi980064a
- Lewis RNAH, McElhaney RN (1998) The structure and organization of phospholipid bilayers as revealed by infrared spectroscopy. *Chem Phys Lipids* 96:9–21. doi:10.1016/S0009-3084(98)00077-2
- Linders LJM, Wolkers WF, Hoekstra FA, van 't Riet K (1997) Effect of added carbohydrates on membrane phase behavior and survival of dried *Lactobacillus plantarum*. *Cryobiology* 35:31–40. doi:10.1006/cryo.1997.2021
- Luzardo MC, Amalfa F, Nuñez AM, Díaz S, Biondi De Lopez AC, Disalvo EA (2000) Effect of trehalose and sucrose on the hydration and dipole potential of lipid bilayers. *Biophys J* 78:2452–2458
- Martos GI, Minahk CJ, Font de Valdez G, Morero R (2007) Effects of protective agents on membrane fluidity of freeze-dried *Lactobacillus delbrueckii* ssp. *bulgaricus*. *Lett Appl Microbiol* 45:282–288. doi:10.1111/j.1472-765X.2007.02188.x
- Mazur P, Leibo SP, Chu EH (1972) A two-factor hypothesis of freezing injury. Evidence from Chinese hamster tissue-culture cells. *Exp Cell Res* 71:345–355
- Molina-Höppner A, Doster W, Vogel RF, Gänzle MG (2004) Protective effect of sucrose and sodium chloride for *Lactococcus lactis* during sublethal and lethal high-pressure treatments. *Appl Environ Microbiol* 70:2013–2020. doi:10.1128/AEM.70.4.2013-2020.2004
- Moussa M, Dumont F, Perrier-Cornet J-M, Gervais P (2008) Cell inactivation and membrane damage after long-term treatments at sub-zero temperature in the supercooled and frozen states. *Biotechnol Bioeng* 101:1245–1255. doi:10.1002/bit.21981
- Passot S, Jamme F, Réfrigiers M, Gautier J, Cenard S, Fonseca F (2014) Synchrotron UV fluorescence microscopy for determining membrane fluidity modification of single bacteria with temperatures. *Biomed Spectrosc Imaging* 3:203–210
- Ragoonanan V, Malsam J, Bond DR, Aksan A (2008) Roles of membrane structure and phase transition on the hyperosmotic stress survival of *Geobacter sulfurreducens*. *Biochim Biophys Acta BBA-Biomembr* 1778:2283–2290. doi:10.1016/j.bbamem.2008.06.006
- Rault A, Béal C, Ghorbal S, Ogier J-C, Bouix M (2007) Multiparametric flow cytometry allows rapid assessment and comparison of lactic acid bacteria viability after freezing and during frozen storage. *Cryobiology* 55:35–43. doi:10.1016/j.cryobiol.2007.04.005
- Santivarangkna C, Higl B, Foerst P (2008) Protection mechanisms of sugars during different stages of preparation process of dried lactic acid starter cultures. *Food Microbiol* 25:429–441. doi:10.1016/j.fm.2007.12.004
- Simonin H, Beney L, Gervais P (2008) Controlling the membrane fluidity of yeasts during coupled thermal and osmotic treatments. *Biotechnol Bioeng* 100:325–333. doi:10.1002/bit.21749
- Simonin H, Bergaoui IM, Perrier-Cornet JM, Gervais P (2015) Cryopreservation of *Escherichia coli* K12TG1: protection from the damaging effects of supercooling by freezing. *Cryobiology* 70:115–121. doi:10.1016/j.cryobiol.2014.12.006
- Smittle RB, Gilliland SE, Speck ML (1972) Death of *Lactobacillus bulgaricus* resulting from liquid nitrogen freezing. *Appl Microbiol* 24:551–554
- Streit F, Delettre J, Corrieu G, Béal C (2008) Acid adaptation of *Lactobacillus delbrueckii* subsp. *bulgaricus* induces physiological responses at membrane and cytosolic levels that improves cryotolerance. *J Appl Microbiol* 105:1071–1080. doi:10.1111/j.1365-2672.2008.03848.x
- Streit F, Athès V, Bchir A, Corrieu G, Béal C (2011) Microfiltration conditions modify *Lactobacillus bulgaricus* cryotolerance in response to physiological changes. *Bioprocess Biosyst Eng* 34:197–204. doi:10.1007/s00449-010-0461-3
- Tourdot-Maréchal R, Gaboriau D, Beney L, Diviès C (2000) Membrane fluidity of stressed cells of *Oenococcus oeni*. *Int J Food Microbiol* 55:269–273. doi:10.1016/S0168-1605(00)00202-6
- Tymczyszyn EE, Gómez-Zavaglia A, Disalvo EA (2005) Influence of the growth at high osmolality on the lipid composition, water permeability and osmotic response of *Lactobacillus bulgaricus*. *Arch Biochem Biophys* 443:66–73. doi:10.1016/j.abb.2005.09.004
- Veerkamp JH (1971) Fatty acid composition of *Bifidobacterium* and *Lactobacillus* strains. *J Bacteriol* 108:861–867
- Velly H, Bouix M, Passot S, Penicaud C, Beinstener H, Ghorbal S, Lieben P, Fonseca F (2014) Cyclopropanation of unsaturated fatty acids and membrane rigidification improve the freeze-drying resistance of *Lactococcus lactis*. *Appl Microbiol Biotechnol* 99:907–918. doi:10.1007/s00253-014-6152-2

- Wang Y, Corrieu G, Béal C (2005) Fermentation pH and temperature influence the cryotolerance of *Lactobacillus acidophilus* RD758. *J Dairy Sci* 88:21–29. doi:[10.3168/jds.S0022-0302\(05\)72658-8](https://doi.org/10.3168/jds.S0022-0302(05)72658-8)
- Wolkers W, Oldenhof H (2015) Use of in situ Fourier transform infrared spectroscopy to study freezing and drying of cells. In: Wolkers WF, Oldenhof H (eds) *Cryopreservation and freeze-drying protocols*. Springer, New York, pp. 147–161
- Wolkers WF, Oldenhof H, Glasmacher B (2010) Dehydrating phospholipid vesicles measured in real-time using ATR Fourier transform infrared spectroscopy. *Cryobiology* 61:108–114. doi:[10.1016/j.cryobiol.2010.06.001](https://doi.org/10.1016/j.cryobiol.2010.06.001)